Chemical Science

ROYAL SOCIETY OF CHEMISTRY

EDGE ARTICLE

View Article Online
View Journal | View Issue

Cite this: *Chem. Sci.*, 2025, **16**, 14109

All publication charges for this article have been paid for by the Royal Society of Chemistry

Synthesis of benzoquinone compounds by a microdroplet-accelerated retro-Diels–Alder reaction†

Nishkant Malkoti,[a] Yifan Meng,[b] Richard N. Zare *[b] and Elumalai Gnanamani*[a]

Received 23rd May 2025
Accepted 2nd July 2025

DOI: 10.1039/d5sc03761a

rsc.li/chemical-science

The unique environment of water microdroplets has enabled several novel organic transformations to be reported in recent years. Given the significance of the retro-Diels–Alder (rDA) reaction in organic and natural product synthesis, we demonstrate a highly accelerated rDA reaction using water microdroplets. The rDA reaction is a reversible process of the classical Diels–Alder cycloaddition, triggered by the dissociation of a six-membered ring, typically under thermal conditions. In this study, Diels–Alder adducts dissolved in water/methanol were electro-sprayed using nitrogen gas at a pressure of 120 psi, leading to efficient rDA product formation of benzoquinones. The products were characterized by mass spectrometry (MS) and tandem mass spectrometry (MS^2). Additionally, crude samples were collected after passage through a 40 mm heated channel (150 °C) for ≈1.2 ms in xylene solvents sprayed under 50 psi for 30 minutes, the distance between sprayer and collection chamber kept at 240 mm. The structures were further confirmed using MS, IR, ^{1}H-NMR, and ^{13}C-NMR analyses. Notably, 2.6 mg of the blue scorpion venom compound, 5-methoxy-2,3-bis(methylthio)cyclohexa-2,5-diene-1,4-dione, was obtained in 60% isolated yield. This compound, originally isolated from scorpion venom, exhibits remarkable antimicrobial activity against *Mycobacterium tuberculosis* and the priority pathogen *Acinetobacter baumannii*. The products were formed within milliseconds, representing a significant rate enhancement compared to traditional bulk-phase rDA reactions.

Introduction

The retro-Diels–Alder (rDA) reaction is a powerful tool in the synthesis of reactive olefins, strained molecules, and metastable molecular entities—structures often challenging to access by conventional synthetic routes.[1–4] Widely applied in synthetic chemistry,[5–7] natural product synthesis,[8–10] and material science,[11–17] the rDA reaction typically requires high temperatures due to its endothermic nature. Consequently, product decomposition and long reaction durations pose significant challenges, and only limited literature reports exist under conventional conditions. Efforts to address these challenges have led to methods like photo-assisted,[18] force-assisted,[19] and microwave-assisted rDA reactions.[20,21] These advances aim to make the rDA reaction more accessible and efficient for synthetic applications. However, easier, cleaner, and faster rDA processes are still highly desirable. We address the limitations of extended reaction times and forcing temperatures by employing microdroplet chemistry that operates under accelerated and milder conditions. Microdroplet reactions have become a promising and rapidly expanding field of research owing to their remarkable ability to accelerate chemical reactions compared to those occurring in the bulk phase.[22–30] The air–water interface creates a distinct environment that diverges significantly from bulk-phase conditions, potentially modifying reaction pathways and mechanistic dynamics. Moreover, phenomena such as droplet evaporation, reagent confinement, and the effect of interfacial electric fields collectively contribute to an acceleration in reaction kinetics. Consequently, these reactions can proceed under milder conditions with lower reagent consumption while achieving highly efficient conversion compared to bulk processes.[31,32] This phenomenon has implications for synthetic chemistry, biochemical processes, and potential industrial applications.

In recent years, the microdroplet technique has been widely utilised for organic transformations. Microdroplet techniques have been used in organic transformations, including addition/elimination, oxidation/reduction, multicomponent reactions, and rearrangements.[33,34] Recently, Xie *et al.* reported the Diels–Alder reaction using microdroplet conditions and further confirmed by MS and DFT calculations.[35] Our group and several other groups established the organic reactions using microdroplet reactions, which enhance the rate, reduce the

[a]*Department of Chemistry, Indian Institute of Technology Roorkee, Roorkee, 247667, India. E-mail: gnanam@cy.iitr.ac.in*

[b]*Department of Chemistry, Stanford University, Stanford, CA 94305-5080, USA. E-mail: zare@stanford.edu*

† Electronic supplementary information (ESI) available. See DOI: https://doi.org/10.1039/d5sc03761a

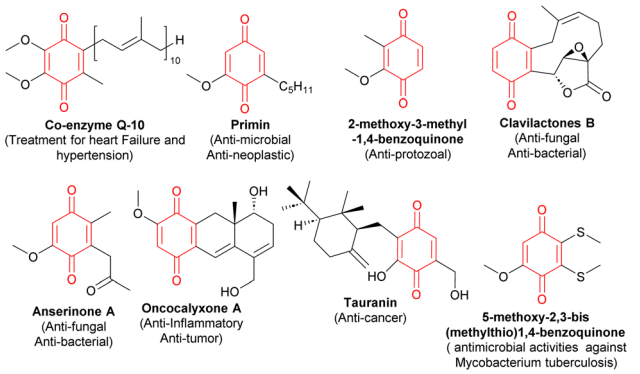

Fig. 1 Representative examples of biologically active compounds having quinone moiety.

temperature, and eliminate the need for added catalysts.[32,36,37a] Interestingly, Zhang *et al.* demonstrated that the microdroplet reactions occur in unactivated droplets.[37b] Although several reports exist for organic transformations in microdroplets, to the best of our knowledge, no report exists for the formation and isolation of benzoquinone compounds under microdroplet conditions.

Several quinone-containing compounds exhibit important biological activities (Fig. 1).[38] For example, coenzyme Q-10 is used to treat heart failure and hypertension;[39,40] primin exhibits antimicrobial and antineoplastic activities;[41,42] 2-methoxy-3-methyl-1,4-benzoquinone shows antiprotozoal activity;[43] anserinone A and clavilactones B have antifungal and antibacterial properties;[44–46] oncocalyxone A possesses anti-inflammatory properties;[47,48] and tauranin acts as an anticancer agent.[49] The blue scorpion venom compound, containing a benzoquinone core, demonstrates notable activity against *Mycobacterium tuberculosis* and the priority pathogen *Acinetobacter baumannii*.[50,51] Because of the high cost of venom extraction, the compound was synthesized in seven steps, with the final step involving an rDA reaction that requires 12 hours. Due to its biological significance, we selected this venom compound as a model substrate for developing the rDA reaction under microdroplet conditions.

Results and discussion

Microdroplets were generated using a sprayer with nitrogen gas as the nebulizing medium. A positive voltage (+4 kV) was applied to enhance the electric field at the water–gas interface and accelerate the reaction. A high-resolution mass spectrometer directly detected the ions from the microdroplets. The distance between the sprayer and MS inlet was maintained at 10 mm. Fig. 2B shows the reaction scheme for the synthesis of 5-methoxy-2,3-bis(methylthio)cyclohexa-2,5-diene-1,4-dione (**2a**) from 4*a*-methoxy-6,7-bis(methylthio)-1,4,4*a*,8*a*-tetrahydro-1,4-methanonaphthalene-5,8-dione (**1a**). To determine a suitable MS solvent, we screened the reaction with various solvents, and the results are shown in Fig. 2C. Aqueous methanol showed an optimal intensity of product formation. This is due to the excellent ionization and stabilization of reactive intermediates in polar solvents. While in nonpolar solvents low conversion has been observed caused by less ionization. Next, we carried out the experiment with different high voltage, and found that conversion increased with 6 kV, without applied voltage, we also observed the product peak with low intensity (Fig. 2D).

Fig. 2E shows the mass spectrum of the chemical content in microdroplets containing the Diels–Alder adduct in a 1 : 1 ratio of methanol/water, in N_2 as the nebulising gas. A peak of mass-to-charge ratio (m/z) at 231.0149 can be clearly observed which indicates the product formation. This peak is identified as the desired protonated rDA product $C_9H_{10}O_3S_2^+$, the calculated exact mass of exact m/z is 231.0144. Further, the product tandem mass (MS^2) analysis is used to confirm the structure of the compound. Fig. 2F shows the MS^2 spectrum of the product peak at m/z 231.0149. The peak of m/z at 215.9911 represents the loss of a methyl group, and two methyl losses appeared at m/z 200.9676. These MS and MS^2 data clearly indicate the formation of the rDA product.

To further confirm the structure using NMR and IR analysis, the DA adduct (**1a**) was sprayed at room temperature in MeOH:H_2O at a 30 μL min^{-1} flow rate under 120 psi pressure of nitrogen gas, and the collected compound was analysed using ^{1}H-NMR, but interestingly, the product was not observed under these conditions; next, a positive voltage (+4 kV) was applied, but the reaction still failed to form the product. This issue may be that the reaction temperature is not sufficient to carry out the reaction. Hence, we customized the setup, which heats the system between the sprayer and the collection flask. We used a high-boiling solvent such as xylene instead of methanol–water. A solution of 0.042 M of **1a** was pneumatically nebulized into microdroplets at a 30 μL min^{-1} flow rate under 75 psi pressure of N_2 gas.

The droplets were passed ≈1.2 ms to the bottom of a 500 mL round-bottom (RB) flask with 50 psi nitrogen gas. The top of the flask is heated to 150 °C by a 40-mm heating coil while the bottom of the flask is at room temperature.[52] In between the heating coil and the collection flask, we attached a heat-resistant foam to avoid thin film reactions in the RB flask (Fig. S1†).[53,54] The distance between sprayer and collecting surface was kept at 240 mm; hence, the total time required for the reaction is ≈7.2 ms at 50 psi pressure. The microdroplet reaction is approximately 6×10^6 times faster than the corresponding bulk reaction (the bulk reaction required 12 h).[50] To collect the larger quantity for the NMR analysis, we sprayed 0.042 M solution of reactant for 30 minutes and collected in room-temperature flask (Fig. 3). Collected microdroplets were subjected to a crude ^{1}H-NMR analysis. From the crude ^{1}H-NMR, it was observed that the rDA was observed with 3% conversion under microdroplet conditions (Fig. 4, entry 1). Also, we screened the reaction with MeOH:H_2O at 120 psi, and no product was observed (Table S1,† entry 1). Further at 75 psi in MeOH:H_2O, we observed 1% of the product. This yield reduction compared to nonpolar solvent is caused by the low-boiling point of MeOH:H_2O solvent and additionally polar solvents react with intermediates which leads to decomposition of the compounds. The lower yield may be caused by the shorter

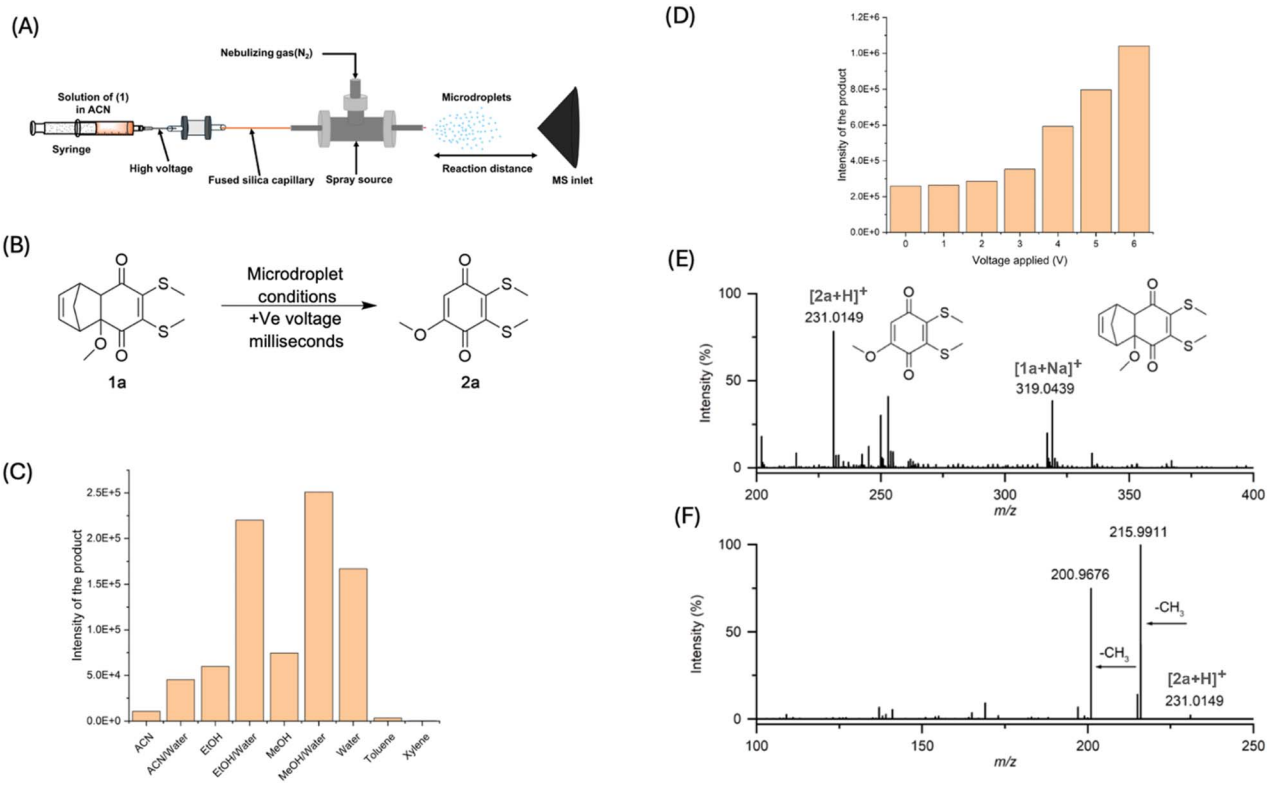

Fig. 2 Synthesis of the blue scorpion venom benzoquinone by microdroplet chemistry. (A) Schematic diagram of the experimental setup using Diels–Alder adduct in ACN. (B) Reaction scheme. (C) Effect of solvent. (D) Applied voltage (at 10 mm reaction distance) on the signal intensity of rDA product (*m*/*z* 231.0149). (E) Mass spectrum of the water microdroplets containing Diels–Alder adduct **1a**. (F) MS^2 spectrum of the product (*m*/*z* 231.0149).

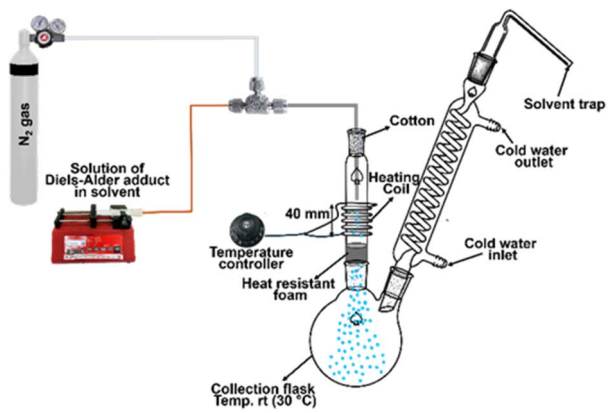

Fig. 3 Schematic diagram of microdroplet setup.

duration of passing the compounds through the heating setup. If the pressure is reduced, the compound may stay longer in the heating region, which may induce the product formation. At 50 psi pressure, as we expected, the product conversion was increased to 21% (Fig. 4, entry 2). To further improve the conversion, we reduced the pressure to 25 psi. Unfortunately, the observed product conversion dropped to 7% (Fig. 4, entry 3). This may be because at low pressure, the size of the microdroplet is higher, which disfavors product formation at the solvent–air interface.

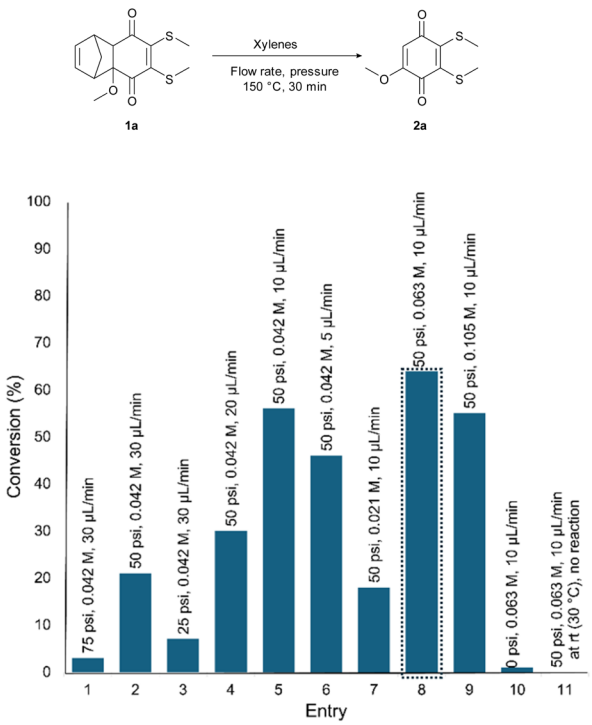

Fig. 4 Optimization of rDA reaction conditions for the synthesis of blue venom compound (best condition boxed).

Pressure plays a significant role in determining the course of the reaction, because it affects both the size of the droplets and the reactivity, keeping in mind that a pressure of 50 psi was optimal. Next, we screened the reaction with various flow rates to further improve the conversion (Fig. 4, entries 4–6). When reducing the flow rate from 30 μL min^{-1} to 20 μL min^{-1}, the yield of product improved from 21% to 30% (Fig. 4, entry 4). These results inspired us to screen other rates, such as 10 μL min^{-1} and 5 μL min^{-1}. While reducing the flow rate further to 10 μL min^{-1} improved conversion to 56%, decreasing it further to 5 μL min^{-1} reduced it slightly to 46% (Fig. 4, entries 5–6). While decreasing the temperature to 120 °C (50 psi with 10 μL min^{-1}) the product conversion drastically reduced to 13% (Table S1,† entry 10). Having optimized flow rate (10 μL min^{-1}), temperature (150 °C) and pressure (50 psi), next we screened the reaction with various solvents, such as toluene, mesitylene, acetonitrile, acetonitrile/water, and DMSO/water (Table S1,† entries 11–15). The nonpolar solvents toluene and mesitylene yielded the corresponding rDA product at 41% and 48% conversion, respectively (Table S1,† entries 11 and 12). With polar solvents, conversion decreased substantially; acetonitrile provided only 11% conversion (Table S1,† entry 13), whereas ACN : water (90 : 10) and DMSO : water (90 : 10) both afforded less than 5% conversion (Table S1,† entries 14–15). The low conversion was observed in polar solvents, caused by solvent evaporation and intermediates reacting with polar solvents in the heated chamber, which leads to side products and decomposition. Hence polar solvents afforded lower reaction yields. We found the best solvent to be xylene. Reducing the concentration of the reaction mixture from 0.042 M to 0.021 M at a flow rate of 10 μL min^{-1} and a pressure of 50 psi decreased conversion to 18% (Fig. 4, entry 7). Increasing the concentration to 0.063 M improved conversion to 64% (Fig. 4, entry 8), while increasing it further to 0.105 M was not beneficial (Fig. 4, entry 9). Based on the extensive optimization, the best conditions were found to be 0.063 M in xylene with 50 psi pressure and 10 μL min^{-1} flow rate (Fig. 4, entry 8). To determine the role of pressure the control experiment was conducted, without pressure (0 psi), trace amount of conversion (<2%) was observed (Fig. 4, entry 10). Similarly, at room temperature no product was observed (Fig. 4, entry 11).

To expand the scope of our developed method, we performed the reaction with various Diels–Alder adducts on a 0.019 mmol scale (Scheme 1) sprayed for 30 min. The compound scorpion venom blue compound 4a-methoxy-6,7-bis(methylthio)-1,4,4a,8a-tetrahydro-1,4-methanonaphthalene-5,8-dione (**1a**) afforded 2.6 mg of **2a** in 60% isolated yield. The dichloro-substituted Diels–Alder adduct **1b** afforded the corresponding rDA product 2,3-dichlorobenzoquinone (**2b**) in 62% yield. Further, we also screened the reaction with the highly chlorine-substituted Diels–Alder adduct **1c**, which gave **2c** in 68% yield. In the case of the trimethyl-substituted adduct **1d**, the corresponding rDA product **2d** was obtained in 58% yield. Owing to the importance of alkyl thioethers in bio-active compounds, we screened the reaction with the propyl mercaptan-containing

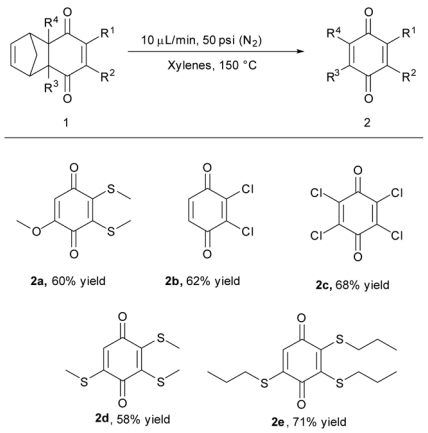

Scheme 1 Substrate scope of retro-Diels–Alder reaction in microdroplets. [a]All the reactions 0.019 mmol of **1** in 0.3 mL of xylenes was sprayed at 150 °C for 30 min. Yields of isolated products are given.

Diels–Alder adduct **1e**, which was also well tolerated and afforded the corresponding product **2e** in a 71% yield.

Conclusions

In summary, we developed an efficient method for the retro-Diels–Alder reaction using the microdroplet technique to achieve accelerated product formation. We customized a new design for high temperature microdroplet reactions. Further, we scaled the process to provide sufficient amounts of material to characterize using NMR and IR. Our approach offers an efficient synthesis of bio-active scorpion venom blue benzoquinone, which shows antimicrobial activity against *Mycobacterium tuberculosis* and the priority pathogen *Acinetobacter baumannii*. The various substituted benzoquinones were obtained in up to 71% yield.

Data availability

The data supporting this article have been included as part of the ESI.†

Author contributions

E. G. and R. N. Z. designed the project and supervised. Experiments were carried out by N. M. and Y. M. The manuscript was written by all authors.

Conflicts of interest

There are no conflicts to declare.

Acknowledgements

This work is supported by the SERB (ANRF), India (SRG/2021/0019070) and Air Force Office of Scientific Research through the Multidisciplinary University Research Initiative (MURI) program (AFOSR FA9550-21-1-0170).

References

1 B. Rickborn, The Retro-Diels-Alder Reaction Part I C-C Dienophiles, *Organic Reactions*, Wiley, 1998.
2 B. Rickborn, The Retro-Diels-Alder Reaction Part II. Dienophiles with One or More Heteroatom, *Organic Reactions*, Wiley, 1998.
3 J. Park, J.-M. Heo, S. Seong, J. Noh and J.-M. Kim, *Nat. Commun.*, 2021, **12**, 4207.
4 Y. Chung, B. F. Duerr, T. A. McKelvey, P. Nanjappan and A. W. Czarnik, *J. Org. Chem.*, 1989, **54**, 1018–1032.
5 R. A. A. Foster and M. C. Willis, *Chem. Soc. Rev.*, 2013, **42**, 63–76.
6 A. L. W. Demuynck, P. Levecque, A. Kidane, D. W. Gammon, E. Sickle, P. A. Jacobs, D. E. De Vos and B. F. Sels, *Adv. Synth. Catal.*, 2010, **352**, 3419–3430.
7 M. Chia, M. A. Haider, G. Pollock III, G. A. Kraus, M. Neurock and J. A. Dumesic, *J. Am. Chem. Soc.*, 2013, **135**, 5699–5708.
8 A. Ichihara, *Synthesis*, 1987, 207–222.
9 A. Ichihara, in *Studies in Natural Products Chemistry*, Elsevier, 2008, pp. 129–171.
10 K. C. Nicolaou, S. A. Snyder, T. Montagnon and G. Vassilikogiannakis, *Angew. Chem., Int. Ed.*, 2002, **41**, 1668–1698.
11 X. Chen, M. A. Dam, K. Ono, A. Mal, H. Shen, S. R. Nutt, K. Sheran and F. Wudl, *Science*, 2002, **295**, 1698–1702.
12 A. Afzali, C. D. Dimitrakopoulos and T. L. Breen, *J. Am. Chem. Soc.*, 2002, **124**, 8812–8813.
13 Y. Adachi, H. Nakagawa, K. Matsuo, T. Suzuki and N. Miyata, *Chem. Commun.*, 2008, 5149–5151.
14 K. Matsuo, H. Nakagawa, Y. Adachi, E. Kameda, H. Tsumoto, T. Suzuki and N. Miyata, *Chem. Commun.*, 2010, **46**, 3788–3790.
15 J. H. Edwards, W. J. Feast and D. C. Bott, *Polymer*, 1984, **25**, 395–398.
16 C. B. Gorman, E. J. Ginsburg and R. H. Grubbs, *J. Am. Chem. Soc.*, 1993, **115**, 1397–1409.
17 R. Tian, Z. Shi and Y. Liao, *Org. Electron.*, 2009, **10**, 368–371.
18 V. K. Johns, Z. Shi, W. Dang, M. D. McInnis, Y. Weng and Y. Liao, *J. Phys. Chem. A*, 2011, **115**, 8093–8099.
19 R. Stevenson and G. De Bo, *J. Am. Chem. Soc.*, 2017, **139**, 16768–16771.
20 S. Dong, K. J. Cahill, M.-I. Kang, N. H. Colburn, C. J. Henrich, J. A. Wilson, J. A. Beutler, R. P. Johnson and J. A. Porco, *J. Org. Chem.*, 2011, **76**, 8944–8954.
21 M. A. Frasso, A. E. Stiegman and G. B. Dudley, *Chem. Commun.*, 2020, **56**, 11247–11250.
22 X. Yan, R. M. Bain and R. G. Cooks, *Angew. Chem., Int. Ed.*, 2016, **55**, 12960–12972.
23 Y. Meng, R. N. Zare and E. Gnanamani, *Angew. Chem., Int. Ed.*, 2024, **63**, e202316131.
24 P. Basuri, L. E. Gonzalez, N. M. Morato, T. Pradeep and R. G. Cooks, *Chem. Sci.*, 2020, **11**, 12686–12694.
25 H. Chen, R. Wang, T. Chiba, K. Foreman, K. Bowen and X. Zhang, *J. Am. Chem. Soc.*, 2024, **146**, 10979–10983.
26 X. Chen, Y. Xia, Y. Yang, Y. Xu, X. Jia, R. N Zare and F. Wang, *J. Am. Chem. Soc.*, 2024, **146**, 29742–29750.
27 L. Xue, B. Zheng, J. Sun, J. Liu and H. Cheng, *ACS Sustain. Chem. Eng.*, 2023, **11**, 12780–12789.
28 Y. Wu, H. Cheng, J. Li, J. Liu and J. Sun, *J. Org. Chem.*, 2023, **88**, 11186–11196.
29 A. Nandy, A. Kumar, S. Mondal, D. Koner and S. Banerjee, *J. Am. Chem. Soc.*, 2023, **145**, 15674–15679.
30 L. Qiu and R. G. Cooks, *Angew. Chem., Int. Ed.*, 2024, **63**, e202400118.
31 S. Chen, K. Dong, J. Sun, M. Ye, J. Liu and H. Cheng, *ACS Sustain. Chem. Eng.*, 2024, **12**, 9522–9533.
32 K. Naveen, V. S. Rawat, R. Verma and E. Gnanamani, *Chem. Commun.*, 2024, **60**, 13263–13266.
33 M. Mofidfar, M. A. Mehrgardi and R. N. Zare, *J. Am. Chem. Soc.*, 2024, **146**, 18498–18503.
34 A. Kumar, S. Mondal and S. Banerjee, *J. Am. Chem. Soc.*, 2021, **143**, 2459–2463.
35 K. Gong, A. Nandy, Z. Song, Q.-S. Li, A. Hassanali, G. Casssone, S. Banerjee and J. Xie, *J. Am. Chem. Soc.*, 2024, **146**, 31585–31596.
36 J. Ghosh, J. Mendoza and R. G. Cooks, *Angew. Chem., Int. Ed.*, 2022, **61**, e202214090.
37 (*a*) H. Chen, R. Wang, T. Chiba, K. Foreman, K. Bowen and X. Zhang, *J. Am. Chem. Soc.*, 2024, **146**, 10979–10983; (*b*) H. Chen, X. Li, B. Li, Y. Chen, H. Ouyang, Y. Li and X. Zhang, *J. Am. Chem. Soc.*, 2025, **147**, 11399–11406.
38 J. L. Bolton and T. Dunlap, *Chem. Res. Toxicol.*, 2017, **30**, 13–37.
39 V. Digiesi, F. Cantini, A. Oradei, G. Bisi, G. C. Guarino, A. Brocchi, F. Bellandi, M. Mancini and G. P. Littarru, *Mol. Aspects Med.*, 1994, **15**, 257–263.
40 R. Belardinelli, A. Muçaj, F. Lacalaprice, M. Solenghi, G. Seddaiu, F. Principi, L. Tiano and G. P. Littarru, *Eur. Heart J.*, 2006, **27**, 2675–2681.
41 E. Bernays, A. Lupi, R. M. Bettolo, C. Mastrofrancesco and P. Tagliatesta, *Experientia*, 1984, **40**, 1010–1011.
42 O. G. Lima, G. B. Marini-Bettolo, F. D. Monache, J. S. d. B. Coelho, L. I. d'Albuquerque, G. M. Maciel, A. Lacerda, D. G. D. Martins, I. V. Albuquerque and G. M. Maciel, *Rev. Inst. Antibiot.*, 1970, **10**, 29.
43 P. J. Weldon, J. R. Aldrich, J. A. Klun, J. E. Oliver and M. Debboun, *Sci. Nat.*, 2003, **90**, 301–304.
44 H. Wang, K. B. Gloer, J. B. Gloer, J. A. Scott and D. Malloch, *J. Nat. Prod.*, 1997, **60**, 629–631.
45 A. Arnone, R. Cardillo, S. V. Meille, G. Nasini and M. Tolazzi, *J. Chem. Soc., Perkin Trans. 1*, 1994, 2165–2168.
46 I. Larrosa, M. I. Da Silva, P. M. Gómez, P. Hannen, E. Ko, S. R. Lenger, S. R. Linke, A. J. P. White, D. Wilton and A. G. M. Barrett, *J. Am. Chem. Soc.*, 2006, **128**, 14042–14043.
47 M. A. D. Ferreira, O. D. R. H. Nunes, J. B. Fontenele, O. D. L. Pessoa, T. L. G. Lemos and G. S. B. Viana, *Phytomedicine*, 2004, **11**, 315–322.
48 A. C. H. Barreto, V. R. Santiago, R. M. Freire, S. E. Mazzetto, J. C. Denardin, G. Mele, I. M. Cavalcante, M. E. N. P. Ribeiro, N. M. P. S. Ricardo, T. Gonçalves, L. Carbone, T. L. G. Lemos,

O. D. L. Pessoa and P. B. A. Fechine, *Int. J. Mol. Sci.*, 2013, **14**, 18269–18283.

49 E. M. K. Wijeratne, P. A. Paranagama, M. T. Marron, M. K. Gunatilaka, A. E. Arnold and A. A. L. Gunatilaka, *J. Nat. Prod.*, 2008, **71**, 218–222.

50 E. N. Carcamo-Noriega, S. Sathyamoorthi, S. Banerjee, E. Gnanamani, M. Mendoza-Trujillo, D. Mata-Espinosa, R. Hernández-Pando, J. I. Veytia-Bucheli, L. D. Possani and R. N. Zare, *Proc. Natl. Acad. Sci. U. S. A.*, 2019, **116**, 12642–12647.

51 R. Gallegos-Monterrosa, J. I. Cid-Uribe, G. Delgado-Prudencio, D. Pérez-Morales, M. M. Banda, A. Téllez-Galván, E. N. Carcamo-Noriega, U. Garza-Ramos, R. N. Zare, L. D. Possani and V. H. Bustamante, *J. Antibiot.*, 2025, **78**, 235–245.

52 J. K. Lee, S. Kim, H. G. Nam and R. N. Zare, *Proc. Natl. Acad. Sci. U. S. A.*, 2015, **112**, 3898–3903.

53 Y. Wu, H. Cheng, J. Li, J. Liu and J. Sun, *J. Org. Chem.*, 2023, **88**, 11186–11196.

54 H. Nie, Z. Wei, L. Qiu, X. Chen, D. T. Holden and R. G. Cooks, *Chem. Sci.*, 2020, **11**, 2356–2361.